

Lasers in Manufacturing Conference 2023

# Manufacturing of transparent quartz glass via laser powder bed fusion

T. Schmidt<sup>a</sup>, C. Scholz<sup>a</sup>, S. Kasch<sup>a,\*</sup>, M. Kahle<sup>a</sup>

<sup>a</sup>*ifw-Jena Günter-Köhler-Institut für Fügetechnik und Werkstoffprüfung, Ernst-Ruska-Ring 3, 07745 Jena, Germany*

---

## Abstract

Recent developments for the additive manufacturing of glass components, the process parameters, the employed system technology and methods of material qualification are presented. The process of laser based powder bed fusion (PBF-LB) – often called selective laser melting as well – for the manufacturing of transparent components from quartz glass powder uses a defocused laser beam for layer-by-layer melting of the glass powder and a focused laser beam for a parallel contour processing during the process. The focused, pulsed laser beam has a higher pulse peak power, and adhering particles in the edge area of the melted component are removed. After the particle edge is removed, the produced samples exhibit relatively low roughness, high transparency and usual density values of fused quartz.

The process will be explained in detail, as well as perspectives and challenges. The PBF-LB process with glass materials will be compared to metals, and properties (roughness, density, stress, accuracy) of produced quartz-glass pieces will be shown.

Keywords: PBF-LB; quartz glass powder; CO<sub>2</sub> laser; laser beam melting; 3D quartz glass components; transparency

---

## 1. Introduction

The material group of glass comprises materials with versatile properties and applications. Depending on the type of glass, the chemical or corrosion resistance, the electrical insulating effect or the low thermal expansion are to be mentioned in addition to the special property of optical transparency. For this reason, glass is used in research and science, as well as in medical technology, chemical and pharmaceutical industries, electrical and electronics industries, and in measurement and sensor technology (Schaeffer 2020). Quartz glass is an indispensable material for many applications due to its high thermal stability up to approx. 1,600 °C, very high resistance to acids, high purity and high light transmission. This is why the industry is interested in expanding manufacturing processes for production.

Additive manufacturing processes enable a rethink in the areas of product development and manufacturing, away from a familiar manufacturing-related product design to a function-integrated individualizable design. For the material groups of plastics and metal, this has already been developed to such an extent that industrial applications are being implemented, and the market is constantly growing and developing. For silicate materials such as glass, however, additive processes, in particular powder-based manufacturing processes are still insufficiently researched, and the plant technology has not yet been sufficiently designed for the requirements of glass processing or has only been introduced in isolated cases on an industrial scale (Gebhardt 2016). Additively manufactured vitreous usually have no or only limited optical transparency and must be reworked.

In the literature, various research approaches are being pursued for the production of three-dimensional glass bodies, which Zhang et al., 2020 or Lachmayer et al., 2020 have summarized. Both conclude that the technological approaches for transparent glass components are still predominantly in a research and development stage. Only a few processes have reached market maturity and these have specific process limitations. Stereolithography enables high-resolution, transparent 3D components and requires subsequent furnace sintering for the glass polymer suspensions used, as described by Kotz et al., 2017. Recent research on this is described by Toombs et al., 2022 as the Computed Axial Lithography (CAL) process, which does not require furnace sintering. However, the process is limited to the size of the building space in which the glass-polymer mixture is processed. Extrusion printing requires a furnace melting chamber and stacks molten glass strand by strand via a nozzle to form 3D components according to Klein et. al., 2015 and Seel et al., 2018. The requirements for machine components that come into contact with glass (mainly soda-lime glass) are very high due to the typically high temperatures of glass. They can contaminate the molten glass and cause impurities. Studies by Witzendorff et al., 2018 and Rettschlag et al., 2020 use quartz glass fibres and CO<sub>2</sub> laser radiation to produce optically transparent components, although the glass strand used is reflected in the component contour. Similar investigations were carried out by Fröhlich et al., 2020 with glass rods made of quartz and borosilicate glass for the multilayer construction of transparent 3D freeforms. However, the structure of the glass strand used (fiber or rod) is reflected in the profile of the glass object in a similar way to the extrusion printing of glass. Schwager et al., 2019 are investigating the powder bed-based, selective laser sintering of glass and present developments in plant technology in conjunction with adapted material systems. Three-dimensional, porous components made of quartz glass powders with densities of 65 % are produced. The research work by Kasch et al., 2020 on laser melting of borosilicate and quartz glass powders presents the different classes of glass powders. They were characterized with regard to geometrical, thermo- and mechanical-physical properties, and the technological processability in the PBF-LB process was investigated using different laser wavelengths. The plant technology was adapted to the increased requirements of glass processing, especially for quartz glass powder with CO<sub>2</sub> laser radiation, and results for melting compact glass samples with transparent properties were presented.

## **2. Process fundamentals and expansion of system technology**

The process chain of selective laser beam melting for glass powder is based on the well-known additive manufacturing processes of powder-bed based laser beam processes for plastic and metal powders. Due to the good absorption of the wavelength of 10.6 µm in the glass, CO<sub>2</sub> lasers of different laser power classes are used. The employed CO<sub>2</sub> laser experimental station was continuously improved during the experimental investigations according to the requirements of powder processing of quartz glass. Two quartz glass powders from QSIL were used, and the geometric properties were characterized. The powder geometry was determined using a scanning electron microscope (SEM) JSM-IT500LA (JEOL). The particle size and its distribution were determined by laser diffraction Mastersizer 3000 (Malvern Panalytical GmbH). Fig. 1 shows

the scanning electron micrographs for the investigated SiO<sub>2</sub> powders with their characteristic fracture grain structure which is due to the production by crushing and grinding molten glass. Table 1 lists essential properties that are necessary for processing in the powder bed. These are on one hand the grain size of the powders for setting the necessary powder layer thickness in the powder bed by the coating process (doctoring) and on the other hand the temperatures of the glass processing for melting with the laser beam. For powder 1 (NC4A), a powder size distribution of 137 μm to 340 μm and for powder 2 (AQP750) of 59 μm to 223 μm was determined. The particle size distributions of the powders correspond to a Gaussian-like distribution, which is also typical for metallic powders in the PBF-LB process. Based on these results, the minimum layer thickness to be applied was experimentally determined to be 300 μm for powder 1 and 200 μm for powder 2.

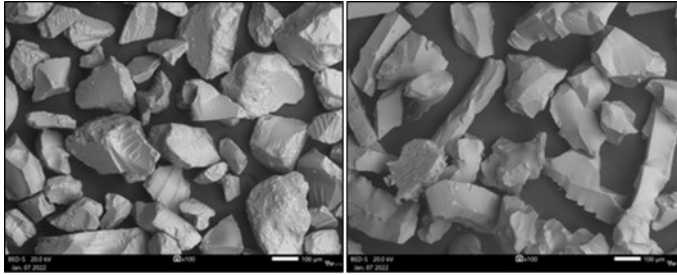


Fig. 1. SEM images of the powders investigated, left: Powder 1 (NC4A) and right: Powder 2 (AQP750).

Table 1. Essential properties of the glass powders.

designation		SiO <sub>2</sub> -powder 1 (NC4A)	SiO <sub>2</sub> -powder 2 (AQP750)
particle size [μm]	MW	235	129
	D10	137	59
	D50	228	105
	D90	340	223
coefficients of expansion α [K <sup>-1</sup> ]		0,5*10 <sup>-6</sup>	0,5*10 <sup>-6</sup>
softening limit T [°C]		1.730	1.715
transformation area T <sub>g</sub> [°C]		1.075 – 1.210	1.075 – 1.210
machining area T [°C]		1.700 – 2.100	1.700 – 2.100
heat conductivity λ [W/m*K]		1,38	1,38

One of the major drawbacks of additive manufacturing with powders is that particles from the powder bed adhere to the component edge and cause a process-related surface roughness. This is also the case when processing glass powders. The adhesion of the glass powder particles and the resulting unevenness or roughness at the specimen edge are shown in Fig. 2. For manufactured glass samples, this means that they do not exhibit continuous optical transparency, as can be seen in Fig. 2 (left). Fig. 2 (right) shows the image of a homogeneously melted, compact glass sample and its edge with adhering glass particles, which is represented by the CT radiographic inspection.

In order to enable both the melting of the particles into a transparent glass and the separation of adhering powder particles in one process sequence, the experimental setup was further developed. This intends to enable the edge processing of the sample contour in one experimental set-up and extends the conventional process sequence of powder bed-based processes for glass according to Fig. 3.

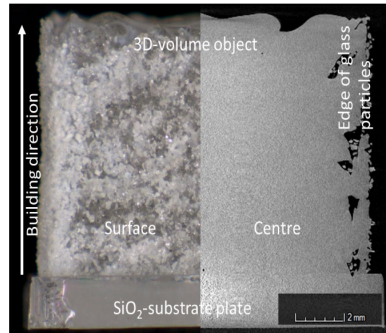


Fig. 2. Illustration of a specimen (10x10x10 mm<sup>3</sup>) made of SiO<sub>2</sub> glass powder. Left: digital microscopy, right: digital radiographic inspection (system XRH222; VisiConsult X-ray Systems & Solutions).

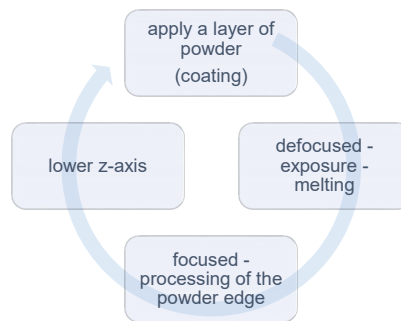


Fig. 3. Developed process flow for glass.

In a first approach, a beam guidance system using two lenses was developed (Fig. 4). The laser beam can be focused by inserting a lens with a focal length of 720 mm. The insertion lens L2 – orange beam path (3) – raises the focus of the scanner optics L1 compared to the blue beam path (2). This ensures that the laser beam is defocused (blue) for melting and focused (orange) for edge processing with higher energy density. The insertion of the L2 lens creates a telescope which shortens the focal length of the L1 scanner optics, given the correct lens spacing (distance between scanner optics and insertion optics) and enables the combination of melting and peripheral processing in one system setup.

Table 2. Design parameters

Abbreviation	Significance
$L_1$	lens 1
$L_2$	lens 2
$H_s$	object-side main plane of the lens system
$H'_s$	image-side main plane of the lens system
AE	working platform
$a$	working distance during powder fusion
$\bar{h}$	distance between lens 1 and object-side main plane of the lens system
$h'$	distance between lens 1 and image-side main plane of the lens system
$f'_s$	focal length of the lens system

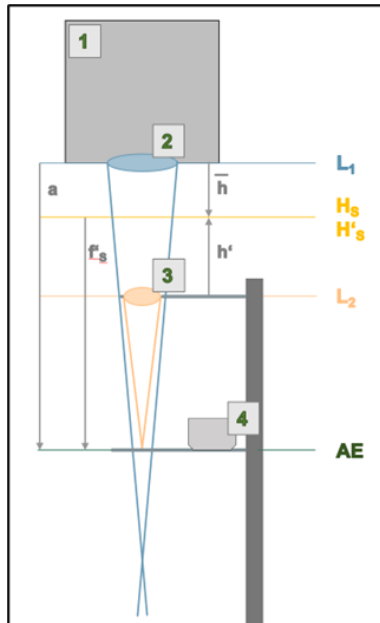


Fig. 4. Simplified schematic representation of the beam guidance and the lens system before (blue - defocused) and after (orange - focused) insertion of the additional lens, 1 scanner | 2 f-theta optics | 3 insertion lens | 4 building platform with powder funnel system.

In order to determine which lens distance is necessary for optimum contour processing, the new beam path was calculated and designed on the basis of the existing optical setup (Table 2). The focusing lens  $L_2$  was installed in the experimental setup at a distance of 60 mm below the scan optics. The process control system performs the change from defocused to focused processing fully automatically according to the programming. This is made possible by the freely assignable inputs and outputs of the scanner control. In this way, the stepper motor for lowering the build plate mold, the two solenoid valves for actuating the pneumatic cylinders for inserting the  $L_2$  lens, and the powder coater receive their control signals at the appropriate points in the program sequence. It is also used to switch the laser from cw mode for melting to pulse mode for peripheral

processing. Integrated limit switches on the L2 lens and coater ensure safe and trouble-free operation of the entire setup.

### 3. Experimental results

The investigations pursue the goal of producing compact, transparent glass bodies using a laser wavelength of 10.6  $\mu\text{m}$  in the PBF-LB process. Using a defined sample contour in the form of a vertical wall (approx. 13 mm x 3 mm), the laser and process parameters for melting and cutting were varied according to Table 3. For melting the quartz glass powder, optimum parameters were determined at a laser power of 120 W and a scanning speed of 45 mm/s in sweep mode, which remained constant during the manufacturing of the specimens. The number of fusion layers varied between 20 and 80 layers, whereas layer thicknesses of 200  $\mu\text{m}$  to 300  $\mu\text{m}$  were investigated according to the employed glass powders. In order to reduce the roughness of the component contour without an additional, external mechanical post-processing step, edge processing was introduced directly after melting each layer. For this purpose, the process sequence according to Fig. 3 and the developed test facility (Fig. 4) were used. In the investigations on edge processing, the laser and process parameters (Table 3) such as laser power, scan speed, loop (number of borders), frequency and duty (duty cycle) were varied after melting the respective layer for a sample. After fabrication, the powder adhesion to the specimen was first visually graded and the degree of detachment evaluated. Samples for which successful edge detachment was possible (Fig. 7) were evaluated with a 3D laser scanning microscope (KEYENCE) for their roughness in comparison to a reference sample without edge detachment.

Table 3. Variation of the essential laser and process parameters.

laser- and process parameters	melting	separating
laser power $P_B$ [W]	100–200	100–500
scan speed $v_{\text{scan}}$ [mm/s]	30–50	5–60
operation mode [Hz]	cw-mode	pulsed mode, 50 – 200
duty cycle [%]	–	3–15
melt layers before border	1–6	–
contour edges (Loop)	–	4–30

Fig. 5 shows the results of the roughness measurement with the corresponding sample numbers, whereby each sample number is assigned to a corresponding laser and process parameter set. In the case of test specimens set up vertically, it was possible to achieve a roughness reduction of more than 18  $\mu\text{m}$  compared to the reference specimen after powder edge removal. The reference surface had a surface roughness of 43  $\mu\text{m}$ . The highest roughness value, from sample T2, was 25  $\mu\text{m}$  and samples T10 and T12 had the lowest roughness value of 11  $\mu\text{m}$ . Thus, the experimental investigations showed that it is possible to reduce the roughness ( $R_a$ ) of the sample contour by approx. 25 %.

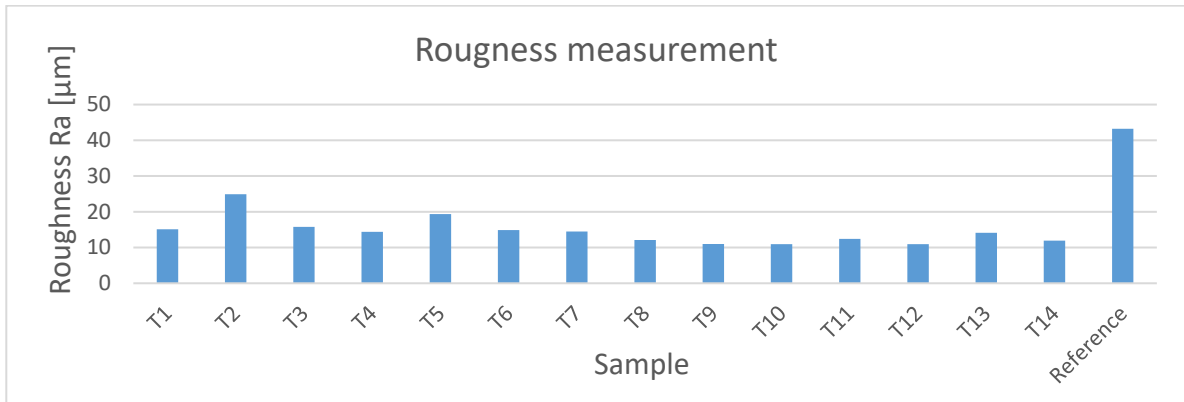


Fig. 5. Evaluation diagram of the roughness measurement.



Fig. 6. (a) rim machining after melting; (b) sample in powder bed after building process; (c) edge detachment after manufacturing.

Fig. 6 shows sections of the manufacturing process. The left picture shows the edge processing during manufacturing. The other two pictures show the finished sample. The middle picture shows the sample in the powder bed and the right picture shows the sample after removal from the powder bed.

Further investigations of the structural formation of the specimen were carried out using digital radiographic testing (VisiConsult). This shows that the PBF-LB process developed can be used to produce compact, transparent glass bodies with minimized roughness and without powder adhesions. Fig. 7 (a) shows the reference sample (Z1) without edge detachment after the melting process. Fig. 7 (b, c) shows sample T10, which was manufactured with the developed test set-up. A compact melt of lowest porosity is clearly visible over the entire sample (Fig. 7, c) and represents a significant improvement of the lateral surface of additively built samples compared to the reference sample. To evaluate the component density, an additional density measurement was carried out according to the Archimedes principle (analytical balance core). A density in the range of  $2.2 \text{ g/cm}^3$  was detected for all tested glass samples, which is comparable to literature values.

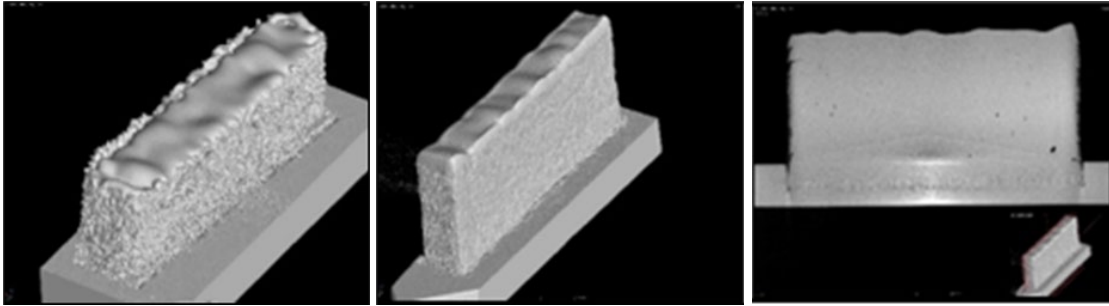


Fig. 7. Photographs of the digital radiographic test; (a) reference sample (10 mm x 4 mm) without edge separation; (b) & (c) sample T10 (15 mm x 3 mm) with edge detachment.

#### 4. Summary and outlook

This paper presents experimental investigations on laser beam powder-bed melting (PBF-LB) of quartz glass powder. The possibility to produce an optically transparent melt as well as the minimization of the contour roughness of manufactured quartz glass samples by means of CO<sub>2</sub> laser radiation was investigated. The system technology was adapted to the various requirements of glass processing. Process parameters for melting and subsequent contour processing in the described system setup were determined and the fundamental minimization of roughness was demonstrated using material engineering methods. As a result of the experiments, parameter windows are available which allow processing of quartz glass powder. The main challenge during edge processing was to keep the heat input into the sample as low as possible. This was achieved by processing the sample contour in laser focus and pulsed laser radiation with higher intensity compared to the melting process. The experiments carried out show that powder edge separation from the homogeneously fused quartz glass, which is transparent in the center, can be implemented without post-processing.

Actual experiments are carried out with a further optimized system technology for melting and edge processing in an experimental station. For example, the optical beam path has been extended by a variable focusing optic, which can focus or defocus the laser beam before it passes through the scanning system. Thus, a variety of focal lengths can be set to produce compact, transparent 3D components made of glass with application-oriented geometries. For future implementation in practice, further experiments are necessary with regard to the laser and process parameters such as pulse frequency, pulse overlap and speed, whereby the overlap of the pulses is decisive for the detachment of the powder edge and must be considered depending on the geometry.

#### 5. Acknowledgements

Parts of the investigations were funded respectively under identifiers IGF 19673 BG and 49MF200150, by the German Federal Ministry of Economic Affairs and Climate Action.



## References

- Fröhlich, F.; Hildebrand, J.; Bergmann, J. P.: Herstellung individueller Strukturen aus silikatischen Werkstoffen mittels Wire-Laser Additive Manufacturing, *Glasbau* 2020, Ernst, Wilhelm & Sohn (2020) 287-297
- Gebhardt, A.: Additive Fertigungsverfahren. Hanser. München (2016). ISBN: 978-3-446-44401-0
- Kasch, S., Schmidt, T., Eichler, F., Thurn, L.-K., Jahn, S. and Brehm, S.: Solution Approaches and Process Concepts for Powder Bed-Based Melting of Glass. AMPA 2020. Springer Nature Switzerland AG 2021. In: Meboldt and Klahn. *Industrializing Additive Manufacturing*, pp.82-95. 2021. [https://doi.org/10.1007/978-3-030-54334-1\\_7](https://doi.org/10.1007/978-3-030-54334-1_7)
- Klein, J., Stern, M., Franchin, G., Kayser, M., Inamura, C., Dave, S., Weaver, J. C., Houk, P., Colombo, P., Yang, M. and Oxman, N.: Additive Manufacturing of Optically Transparent Glass. 2015. Mary Ann Liebert, Inc.
- Kotz, F., Arnold, K., Bauer, W., Schild, D., Keller, N., Sachsenheimer, K., Nargang, T. M., Richter, C., Helmer, D., Rapp, B. H.: Three-dimensional printing of transparent fused silica glass: 2017 *Nature* 544(7650):337-339. <https://doi.org/10.1038/nature22061>
- Lachmayer, R.; Rettschlag, K.; Kaierle, S.: Konstruktion für die Additive Fertigung 2020. Springer Vieweg. (2021). ISBN 978-3-662-63029-7
- Rettschlag, K. et al.: Laser glaa deposition of spheres for printing micro lenses. 11th CIRP Conference on Photonic Technologies [LANE 2020]. 10.1016/j.procir.2020.09.052
- Schaeffer, H. A., Langfeld. R.: Werkstoff Glas – Alter Werkstoff mit Zukunft. Springer Berlin, Heidelberg (2020). <https://doi.org/10.1007/978-3-662-60260-7>
- Schwager, A.-M., Dellith, J., Bruder, A., Baierl, H., Lasch, P., Barz, A., Bliedtner, J., Reichel, V., Rädlein, E.: Hochtemperatur-Laserstrahlsintern von Glaspulverwerkstoffen. Tagungsband zur 11. Mittweidaer Lasertagung, 2019 ISSN 1437-7624
- Seel, M., Akerboom, R., Knaack, U., Oechsner, M., Hof, P. Schneider, J.: Additive Manufacturing of Glass Components - Exploring the Potential of Glass Connections by Fused Deposition Modeling. 2018. ISBN 978-94-6366-044-0, <https://doi.org/10.7480/cgc.6.2161>
- Toombs, J., Luitz, M., Cook, C., Jenne, S., Chung, C., Rapp, Kotz-Helmer, F., Taylor, H.: Volumetric Additive Manufacturing of Silica Glass with Microscale Computed Axial Lithography, <https://arxiv.org/ftp/arxiv/papers/2110/2110.01651.pdf>
- Witzendorff, P; et al.: Additive manufacturing of glass. CO2-Laser glass deposition printing. *Proc. CIRP.* (2018). <https://doi.org/10.1016/j.procir.2018.08.109>
- Zhang, D., Liu, X., Qui, J.: 3D printing of glass by additive manufacturing techniques: a review. 2020. *Front. Optoelectron.* <https://doi.org/10.1007/s12200-020-1009-z>